© 2015. Published by The Company of Biologists Ltd | Journal of Experimental Biology (2015) 218, 3468-3477 doi:10.1242/jeb.129486

RESEARCH ARTICLE

The impact of high-salt exposure on cardiovascular development in the early chick embryo

Guang Wang[1,*], Nuan Zhang[1,*], Yi-Fan Wei[1,*], Yi-Mei Jin[1], Shi-Yao Zhang[1], Xin Cheng[1], Zheng-Lai Ma[1], Shu-Zhu Zhao[1], You-Peng Chen[2], Manli Chuai[3], Berthold Hocher[2,4,‡] and Xuesong Yang[1,5,‡]

ABSTRACT

In this study, we show that high-salt exposure dramatically increases chick mortality during embryo development. As embryonic mortality at early stages mainly results from defects in cardiovascular development, we focused on heart formation and angiogenesis. We found that high-salt exposure enhanced the risk of abnormal heart tube looping and blood congestion in the heart chamber. In the presence of high salt, both ventricular cell proliferation and apoptosis increased. The high osmolarity induced by high salt in the ventricular cardiomyocytes resulted in incomplete differentiation, which might be due to reduced expression of Nkx2.5 and GATA4. Blood vessel density and diameter were suppressed by exposure to high salt in both the yolk sac membrane (YSM) and chorioallantoic membrane models. In addition, high-salt-induced suppression of angiogenesis occurred even at the vasculogenesis stage, as blood island formation was also inhibited by high-salt exposure. At the same time, cell proliferation was repressed and cell apoptosis was enhanced by high-salt exposure in YSM tissue. Moreover, the reduction in expression of *HIF2* and *FGF2* genes might cause high-salt-suppressed angiogenesis. Interestingly, we show that high-salt exposure causes excess generation of reactive oxygen species (ROS) in the heart and YSM tissues, which could be partially rescued through the addition of antioxidants. In total, our study suggests that excess generation of ROS might play an important role in high-salt-induced defects in heart and angiogenesis.

KEY WORDS: High salt/osmolarity, Heart formation, Angiogenesis, ROS

INTRODUCTION

The cardiovascular system is the first system to emerge during embryonic development because it is responsible for distributing the blood supply to various tissues according to their requirements. The cardiovascular system is composed of the heart and the vascular system, which derive from both the embryonic mesoderm and the extraembryonic yolk sac. During early embryonic development, the heart initially forms in an embryonic disc as a simple paired heart tube inside the forming pericardial cavity. In this period, heart formation undergoes a series of transformations, starting from the formation of a straight heart tube deriving from the fusion of bilateral cardiomyogenesis cells in the primary/secondary heart fields on the embryonic midline (Yutzey and Kirby, 2002) and followed by the right looping of the heart tube and septation (Linask, 2003). Endoderm-derived signals such as bone morphogenetic protein (BMP), fibroblast growth factor (FGF) and Wnt antagonists are essential for precardiac mesoderm cells to differentiate into mature cardiomyocytes (Nakajima et al., 2009; Schultheiss et al., 1995) during cardiomyogenesis. Nkx2.5, GATA factors, myocardin and Tbx20 are well-known transcription factors that characterize and induce cardiogenic differentiation (Brand, 2003). Therefore, Nkx2.5 and BMP2 could be considered common cardiogenic factors.

Vascular development occurs in many regions as the mesoderm differentiates into blood islands. The blood islands then contribute to both the blood vessel epithelium and fetal red blood cells. Eventually, these blood islands join together to form the primary blood plexus that connects with the forming heart tube. Angiogenesis is thought to remodel and expand the vascular plexus through endothelial sprouting and intussusceptive microvascular growth (Patan, 2004). Located in the extra-embryonic region, the yolk sac membrane (YSM) is the first site where blood vessels and angioblasts develop. Its physiological function is to provide nutrition to the developing embryo. The chick chorioallantoic membrane (CAM) is a highly vascularized membrane underneath the inner surface of the eggshell. It is formed by the fusion of the chorionic membrane and the allantois during embryonic development. Both the YSM and CAM are excellent models for studying angiogenesis because they are easy to access and manipulate. There is an extensive literature about the genetic background, and the molecular and cellular mechanisms responsible for blood vessel formation during embryonic development. Fibroblast growth factor-2 (FGF2) and vascular endothelial growth factor (VEGF) play an important role in the angiogenic expansion of the early network (Marinaccio et al., 2013). Hypoxia activates hypoxia inducible factor-1 and 2-alpha (HIF-1α and HIF-2α) and could induce vessels to branch towards the hypoxic tissue (Pugh and Ratcliffe, 2003). Reactive oxygen species (ROS), as a component of oxidative phosphorylation, also play an important role in regulation of HIF-1α (Hagen, 2012), VEGF (Xia et al., 2007), FGF2 (Wang et al., 2015b), cardiovascular system (Brown and Griendling, 2015) and embryonic development (Dennery, 2007).

Chick embryos can easily be exposed to salt solutions, making them good models for analyzing the effects of hyperosmolarity on development. The early chick embryos are quite sensitive to external physiochemical compounds. In contrast to the growing mammalian embryo, salt exposure to the chick embryo is a pure high-salt osmolality model; in contrast to the situation in mammals, salt cannot be excreted by the chicken embryo, nor is there a prominent activation of a salt- and osmolality-regulating system

[1]Key Laboratory for Regenerative Medicine of the Ministry of Education, Division of Histology and Embryology, Medical College, Jinan University, Guangzhou 510632, China. [2]Department of Neonates, The first Affiliated Hospital of Jinan University, Guangzhou 510632, China. [3]Division of Cell and Developmental Biology, University of Dundee, Dundee DD1 5EH, UK. [4]Humboldt University of Berlin, University Hospital Charité, Center for Cardiovascular Research & Institute for Pharmacology, Hessischestrasse 3-4, Berlin D-10115, Germany. [5]Institute of Fetal-Preterm Labor Medicine, Jinan University, Guangzhou 510632, China.
*These authors contributed equally to this work

‡Authors for correspondence (yang_xuesong@126.com; berthold.hocher@charite.de)

Received 1 August 2015; Accepted 1 September 2015

Journal of Experimental Biology

Journal of Experimental Biology (2015) 218, 3468-3477 doi:10.1242/jeb.129486

such as the anti-diuretic hormone (ADH) system and the renin–angiotensin–aldosterone system (RAAS). This represents one kind of strength and a weakness of the model. In our previous study, we demonstrated that chick embryos exposed to excess salt have impaired retina and lens development (Chen et al., 2014) and induced neural tube defects (Jin et al., 2015). Here, we investigate the adverse impact of high-salt-induced hyperosmolarity on cardiovascular development using early chick embryos.

MATERIALS AND METHODS

Chick embryos

Fertilized chicken eggs were obtained from the Avian Farm of the South China Agriculture University. The eggs were incubated in a humidified incubator (Yiheng Instrument, Shanghai, China) at 38°C and 70% humidity. After 36 h of incubation, the chick embryos were treated as previously described (Chen et al., 2014; Jin et al., 2015): in brief, 2 ml albumen was removed from an egg and the egg was then injected with 500 µl of three different concentrations of NaCl. For the control group, we injected 0.7% NaCl (calculated final osmolality of the egg was 240 mosm l^{-1}); for the 300 mosm l^{-1} group, we injected 16.85% NaCl (calculated final osmolality of the egg, 300 mosm l^{-1}); for the vitamin C (VC) rescue experiment (Li et al., 2014), we administered VC (0.5 mg egg^{-1}) after injection of 16.85% NaCl. The treated embryos were incubated for a further 72 h. For treatment of the CAM, we injected either simple saline (500 µl of 0.7% salt solution) or high-salt solution (500 µl of 16.85% salt solution) to the blunt side of the egg at day 6. The treated embryos were incubated for a further 48 h. The embryos were firstly determined to be alive or dead by the presence/absence of a heartbeat. Surviving embryos were harvested for assessment of other parameters. All dead embryos were excluded from further analysis.

Histology

Hematoxylin and Eosin staining (H&E staining) was performed on the corresponding transverse embryonic sections [including embryonic day (E) 4.5 chick embryos, E4.5 YSM and E8.0 CAM] according to standard protocols. The thickness of the ventricular walls and the length and number of blood vessels were then measured. Ventricular wall thickness was measured across the transverse plane of the chick ventricular wall from the outer surface to the cardiac lumen at five different points. The trabecular muscle thickness was measured similarly. Blood vessel length and number were measured on the transverse sections of chick YSM. To assess blood vessel density, the blood vessels around the hearts were photographed using a stereomicroscope (Olympus MVX10) and an OPTPRO 2007 image acquisition system. The blood vessel plexus in the same location in the hearts was quantified using an IPP 5.0 image analysis program.

Immunostaining

Chick embryos were harvested after high-salt exposure and fixed in 4% paraformaldehyde (PFA) overnight at 4°C. Whole-mount chick embryo immunostaining was performed using MF20 or phospho-histone H3 (PH3). Briefly, the embryos were washed in phosphate-buffered saline (PBS) and incubated with a primary monoclonal antibody mixture raised against MF20 (1:200, DSHB) or PH3 (1:400, Santa Cruz Biotechnology) overnight at 4°C on a shaker. After extensive rinsing in PBS, the embryos were incubated with Alexa Fluor 555 anti-mouse IgG or anti-rabbit IgG secondary antibody (1:1000, Invitrogen, USA), respectively, at 4°C overnight on a shaker. All embryos were later counterstained with DAPI (1:1000, Invitrogen) at room temperature for 1 h. All immunofluorescence staining was performed in replicate from at least 5–6 embryos

Blood island formation in chick embryos

High-salinity culture [1.125% NaCl:albumen (1:1); calculated final osmolality of the culture, 300 mosm l^{-1}] was applied to one side of stage HH3 onwards chick embryos during early chicken (EC) culture as previously described (He et al., 2013, 2014; Wang et al., 2015a). The other side of embryos treated with simple saline served as the control [0.7% NaCl: albumen (1:1); calculated final osmolality of the culture, 300 mosm l^{-1}] (Chapman et al., 2001). Whole-mount *in situ* hybridization of chick embryos was performed according to standard *in situ* hybridization protocols (Henrique et al., 1995). Digoxigenin-labeled probes were synthesized against VE-cadherin (Yang et al., 2008). The whole-mount stained embryos were photographed and frozen sections were prepared by sectioning at a thickness of 15–20 µm on a cryostat microtome (Leica CM1900).

BrdU incorporation experiments

BrdU stock solution (10 mmol l^{-1}, 10 µl) was administered to high-salt treatment or control eggs/chick embryos 4 h before the embryos reached 4.5 days. Transverse sections of E4.5 chick hearts were stained with a monoclonal antibody against BrdU according to the manufacturer's instructions (Roche). Cell counts were performed from a defined area (visual field at 20× magnification). We counted BrdU-positive cells and the total cell number to calculate the proliferation index (BrdU-positive cells/total cell number).

TUNEL staining

The hearts of E4.5 chicken embryos were fixed in Bouin's solution and paraffin embedded. Sections (4 µm) were deparaffinized and stained with an *in situ* cell death detection kit (Roche) according to the manufacturer's instructions. The extent of cell death was quantified by counting $TUNEL^+$ cells on consecutive transverse sections of treated and untreated E4.5 chick embryonic hearts and YSM. We counted the TUNEL-positive cells and the total cell number to calculate the apoptotic index (TUNEL-positive cells/total cell number).

Cell culture and measurement of intracellular ROS

Human umbilical vascular endothelial cells (HUVECs) were cultured in a humidified incubator at 37°C and 5% CO_2 inside 96-well plates. The cells (1×10^6 cells ml^{-1}) were maintained in DMEM (Gibco, USA) plus 10% fetal bovine serum (Gibco, Australia). 1 ml of 16.85% NaCl (high osmolarity) or 1 ml 0.7% NaCl (control) were added to the 100 ml HUVEC cultures. Levels of intracellular ROS were determined using a non-fluorescent dye DCF-DA (2′,7′-dichlorodihydrofluorescein diacetate) (Sigma-Aldrich), which is oxidized by ROS generated by cells into a fluorescent dye DCF (2′,7′-dichlorofluorescin). The control and high-salt-treated HUVECs were incubated in the presence of 10 µmol l^{-1} DCF-DA for 20 min. The fluorescence intensity was measured using a BD FACSAria.

RNA isolation and RT-PCR

Total RNA was isolated from chick heart and YSM tissues using TRIzol (Invitrogen, USA) according to the manufacturer's instructions. First-strand cDNA was synthesized to a final volume of 25 µl using the SuperScript RIII first-strand synthesis system (Invitrogen, USA). Following reverse transcription, PCR amplification of the cDNA was performed as described previously (Dugaiczyk et al., 1983; Maroto et al., 1997). The primers were as follows: *PPIA*, TGACAAGGTGCCCATAACAG and GCGTAAAGTCACCACCCTGA; cyclin D1, TCGGTGTCCTACTTCA-AGTG and GGAGTTGTCGGTGTAAATGC (Scott-Drechsel et al., 2013); *VMHC*, GCTACAAACACCAAGCAGAG and TCTTATATCTGGGAG-CCAGG (Schlueter et al., 2006); *Nkx2.5*, GGATCCCTCCTCGTTGCTC-TCG and CCTTGACACGCCGCTCTGACTT (Schlueter et al., 2006); *GATA4*, CCACACGACCACAACCACACTCTG and AAAGCTTCAGG-GCTGAAATTGCAG (Zhang et al., 2003); *BMP2*, AGCGTCAAGCGA-AACACAAACAG and GGGCAACAATCCAGTCATTCCAC (Endo et al., 2012); *HIF2*, CCGAGCGTGACTTCTTCATGAGG and GCTCATCGT-CAACAGGTGTGGCT (Larger et al., 2004); FGF2, TTCTTCCTGCGC-ATCAAC and GGATAGCTTTCTGTCCAG (Larger et al., 2004); *VEGFR*, GGTCGCATGAACATGAAGAA and TTGGTAGGGTTTGTAAGGAC; *SOD1*, AGGAGTGGCAGAAGTAG and CACGGAAGAGCAAGTA; *SOD2*, CTTCCTGACCTGCCTTAC and CGTCCCTGCTCCTTATT; *Gpx*, GCCACCTCCATCTACGAC and TGCTCCTTCAGCCACTTC. PCR reactions were performed in a Bio-Rad S1000TM thermal cycler (Bio-Rad, USA). The final reaction volume was 50 µl, composed of 1 µl first-strand cDNA, 25 µmol l^{-1} forward primer, 25 µmol l^{-1} reverse primer, 10 µl PrimeSTARTM Buffer (Mg^{2+} plus), 4 µl dNTPs mixture (TaKaRa, Japan), 0.5 µl PrimeSTARTM HS DNA Polymerase (2.5 U μl^{-1}; TaKaRa, Japan), and RNase-free water to 50 µl. The cDNAs were amplified for

Journal of Experimental Biology (2015) 218, 3468-3477 doi:10.1242/jeb.129486

30 cycles. One round of amplification was performed at 94°C for 30 s, 58°C for 30 s and 72°C for 30 s. The PCR products (20 µl) were resolved in 1% agarose gels (Biowest, Spain) in 1× TAE buffer (0.04 mol l^{-1} Tris acetate and 0.001 mol l^{-1} EDTA) and 10,000× GeneGreen Nucleic Acid Dye (Tiangen, China) solution. The resolved products were visualized with a transilluminator (Syngene, UK), and photographs were captured using a computer-assisted gel documentation system (Syngene). The housekeeping gene *PPIA* (peptidylprolyl isomerase A) was run in parallel to confirm that equal amounts of RNA were used in each reaction. The ratio between intensity of the fluorescently stained bands corresponding to genes and *PPIA* was calculated to quantify the level of the transcripts for those mRNAs (De Simone et al., 2005; Wang et al., 2015a). The RT-PCR result was representative of four independent experiments.

Photography

Following immunohistochemistry, whole-mount embryos were photographed using a stereo-fluorescent microscope (Olympus MVX10) associated with the Olympus software package Image-Pro Plus 7.0. The embryos were sectioned into 15 µm slices using a cryostat microtome (Leica CM1900) and then photographed using an epifluorescent microscope (Olympus LX51, Leica DM 4000B) with a CN4000 FISH Olympus software package.

Data analysis

The assays of blood islands density and blood vessel density (BVD) were performed according to the previous description (Chen et al., 2014; He et al., 2013). Data analyses and creation of charts were performed using a GraphPad Prism 5 software package (GraphPad Software, CA, USA). The data were presented as the mean±s.d. Statistical significances were determined using a non-parametric test. $P<0.05$ was considered to be significant.

RESULTS

High-salt exposure leads to embryonic lethality and heart dysplasia in E4.5 chick embryos

In our previous experiments investigating the influence of high-salt exposure on eye and neural tube development (Chen et al., 2014), we found embryonic lethality. In this study, we carefully tracked the possible mechanisms underlying the embryonic lethality. To mimic a high-salt environment, 500 µl of 16.85% salt solution or simple saline (0.7%, control) was injected into fertilized eggs through the eggshell window (Fig. 1A). Thus, the final osmolarity surrounding the developing embryos was 300 mOsm in the high-salt group (N=30) and 240 mOsm in the control group (N=10). The treated eggs were incubated for 4.5 days. After 4.5 days, 20 out of 30 embryos were dead after the high-salt exposure (Fig. 1E).

The cardiovascular system is the first organ system to develop, as subsequent embryonic development relies on its physiological function. Severe embryonic heart defects could therefore cause embryonic death. We first compared the developing hearts of the control (240 mOsm, Fig. 1B) and high osmolarity (300 mOsm, Fig. 1C,D) embryos. We found two abnormal heart development phenotypes in E4.5 chick embryos in the high-salt group (Fig. 1C,D) compared with control embryos (Fig. 1B). In the control embryonic heart (N=10; Fig. 1B), we clearly saw the appearance of the fully looped heart, while either abnormal looping of heart tube (28%, N=29; Fig. 1C) or blood congestion (17%, N=29; Fig. 1D) occurred in the high-salt-exposed groups (the rate of embryo malformation was established by determining the ratio of abnormal embryo numbers to the total surviving embryo numbers). However, the incidence of heart malformation was not high (Fig. 1F; dead embryos were excluded from analysis). By viewing the transverse sections of these hearts, we also saw abnormal development of the atrium and ventricle (ventricle is still nearer to rostral part than atrium of chick embryo; Fig. 1C1–C3) or excessive numbers of blood cells in the heart chambers (Fig. 1D1–D3), compared with control heart sections (Fig. 1B1–B3).

High-salt exposure affects the normal development of the early heart in E4.5 chick embryos

Next, we measured cardiomyocyte proliferation and apoptosis with BrdU incorporation and TUNEL assays (Fig. 2). Compared with

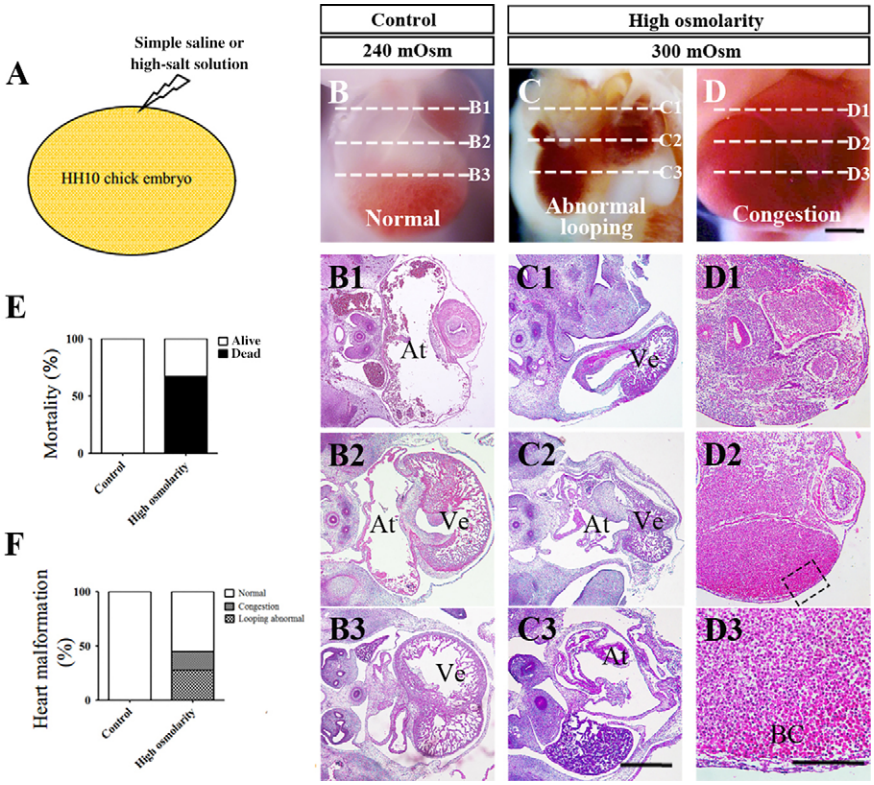

Fig. 1. Morphological alteration of developing E4.5 chick embryonic hearts induced by high-salt exposure. (A) Fertilized chick eggs were exposed to 0.7% NaCl (control) or 300 mOsm l^{-1} NaCl (high osmolarity) for 3 days. (B) Representative appearance of the developing hearts in the control group. (C,D) Examples showing appearance of developing hearts in the high-salt-exposed (300 mOsm) group. In B–D, transverse sections 1–3 were taken at the sites indicated by dashed lines. D3 is an enlargement of boxed region in D2. (E) Bar graph showing the death rate of embryos following high-salt exposure (N=30 embryos in each group). (F) Bar graph showing the occurrence of abnormal hearts in embryos following high-salt exposure (control: N=10 embryos; high osmolarity: N=29 embryos). At, atrium; Ve, ventricle; BC, blood cell. Scale bars: 500 µm (B–D), 400 µm (B1–C3,D1,D2) and 100 µm (D3).

Journal of Experimental Biology

Journal of Experimental Biology (2015) 218, 3468-3477 doi:10.1242/jeb.129486

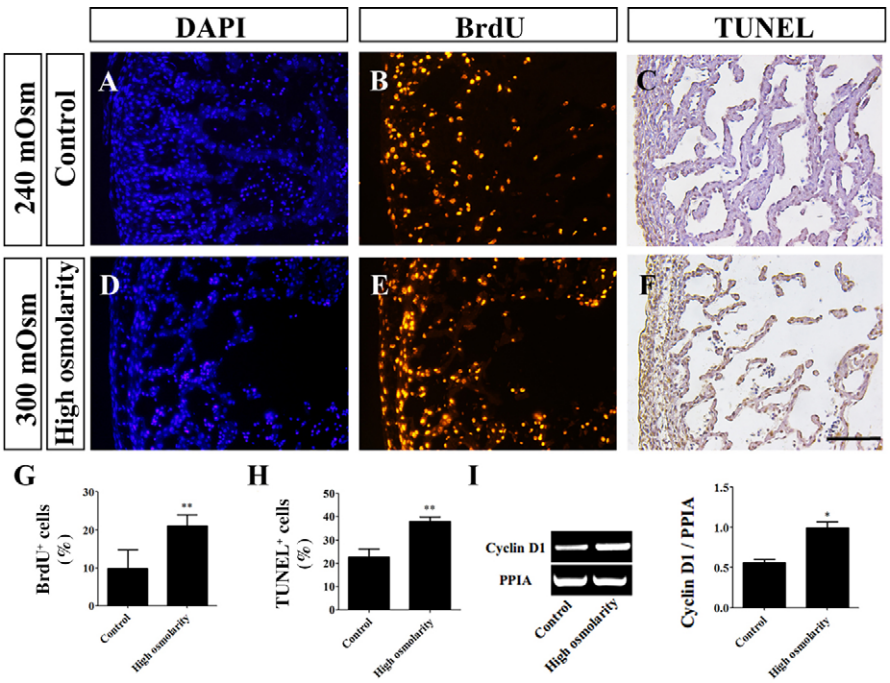

Fig. 2. The impact of high-salt exposure on cell proliferation and apoptosis in embryonic myocardial cells. Fertilized chick eggs were exposed to 240 mOsm l^{-1} (control) and 300 mOsm l^{-1} NaCl (high salt) for 3 days as described above. DAPI staining (A,D), BrdU immunofluorescent staining (B,E) and TUNEL staining (C,F) were performed in serial transverse sections of E4.5 chick embryonic hearts exposed to 240 mOsm l^{-1} (control) or 300 mOsm l^{-1} NaCl (high osmolarity). (G) Bar graph comparing the number of BrdU-positive cells between the control and high-salt exposure groups. (H) Bar graph comparing the number of TUNEL-positive cells between the control and high-salt exposure groups. (I) Semi-quantitative RT-PCR was performed to detect expression of cyclin D1 mRNA in the developing chick hearts after the high osmolarity treatment. Scale bars: 50 µm (A–F).

the control (Fig. 2B), the BrdU-positive cell number was higher in the high-salt-exposed ventricular walls (control=9.82±4.96%, *N*=11; high osmolarity=21.14±7.31%, *N*=7; *P*<0.01; Fig. 2E,G), suggesting that cell proliferation was activated in cardiomyocytes. This outcome is not due to reduced cardiomyocyte numbers in the high-salt-exposed ventricles, because the DAPI staining revealed more cells in the control ventricle walls than in the high-salt-exposed group (Fig. 2A,D). The mRNA expression of cyclin D1, a nuclear protein required for cell cycle progression in G1, was up-regulated nearly two-fold (control=0.56±0.04, high osmolarity=0.99±0.07, *N*=4; *P*<0.01; Fig. 2I), which also suggests that high osmolarity induced by high salt promoted cell proliferation in embryonic cardiomyocytes. Interestingly, TUNEL staining showed that cell apoptosis in the ventricular wall was also significantly promoted by high salt exposure (Fig. 2F) compared with the control (Fig. 2C) (control=22.68±3.57%, *N*=6; high osmolarity=37.85±5.72%, *N*=8; *P*<0.01; Fig. 2H).

To further investigate early heart development, transverse sections from control and high-salt-exposed hearts were generated at the level across the atrium and ventricle (Fig. 3A,B). The measurement of the thickness of the ventricular walls (control=55.87±5.18 µm, *N*=10; high osmolarity=31.94±8.71 µm, *N*=14; *P*<0.001) and the trabecular muscles (control=22.62±3.23 µm, *N*=10; high osmolarity=14.57±2.75 µm, *N*=14; *P*<0.001) showed that both were reduced in high-salt-exposed hearts (Fig. 3D) compared with control hearts (Fig. 3C,G,H). Because the MF20 monoclonal antibody recognizes the myosin II heavy chain in cardiac and skeletal muscles, we used it to examine cardiomyocyte differentiation following high-salt treatment. MF20 was expressed in nearly all the ventricular wall and trabecular muscles in the control hearts (Fig. 3E,E1). However, only some of the ventricular wall and trabecular muscles were MF20 positive in the high-salt-exposed hearts (Fig. 3F,F1), suggesting that cardiomyocyte differentiation was affected by high-salt exposure. We next investigated expression of crucial genes during heart tube development, including *VMHC*, *Nkx2.5*, *GATA4* and *BMP2* using PT-PCR. *VMHC*, *Nkx2.5* and *GATA4* were down-regulated and *BMP2* was not affected by high-salt exposure (*VMHC*/*PPIA*: control=0.88±0.08, high osmolarity=0.41±0.11, *P*<0.05; *Nkx2.5*/*PPIA*: control=0.46±0.04, high osmolarity=0.08±0.02, *P*<0.05; *GATA4*/*PPIA*: control=0.55±0.07, high osmolarity=0.20±0.07, *P*<0.05; *BMP2*/*PPIA*: control=0.99±0.38, high osmolarity=1.36±0.67, *P*>0.05; *N*=4; Fig. 3I). This experimental evidence indicated that high-salt exposure negatively influenced cardiomyocyte differentiation during heart formation.

Inhibitory effects of high-salt exposure on angiogenesis in the yolk sac membrane of chick embryos

We next asked whether angiogenesis was normal in a high-salt environment. High-salt solution was administered to embryos and the chick YSM model in the extraembryonic area opaca was studied, as it is the earliest region of angiogenesis and can be easily manipulated. We examined the development of blood plexuses at the same localization in yolk sac membranes (YSMs) from control (Fig. 4A) and high-salt-exposed (Fig. 4B) embryos. The blood vessel density was lower in the presence of high salt than in the control (control=9.02±1.02%, *N*=9; high osmolarity=5.38±0.96%, *N*=20; *P*<0.001; Fig. 4G). Blood plexus development in the yolk sac membrane occurs not only in two dimensions, but also protrudes into the yolk. Thus, we compared the blood vessels in transverse sections from the same locations of the YSM and found that both the number and diameter of blood vessels in the control YSM sections (Fig. 4C,E) were obviously greater than in the YSM of high-salt-exposed (Fig. 4D,F) embryos (diameter: control=809.91±112.41 µm, *N*=10; high osmolarity=518.63±128.61 µm, *N*=20; number: control=6.40±1.51, *N*=10; high osmolarity=3.47±1.31, *N*=19; *P*<0.001; Fig. 4H,I). These data suggested that high-salt exposure inhibited angiogenesis in YSMs.

We next studied whether cell proliferation (PH3) or apoptosis (TUNEL) contributed to the decreased angiogenesis induced by high-salt exposure. The PH3 immunofluorescent staining was performed in serial sections as in Fig. 4 for both control (Fig. 5A) and high-salt-exposed embryos (Fig. 5B). There were fewer PH3-positive cells in high-salt-exposed embryos (Fig. 5D,F) than

Journal of Experimental Biology (2015) 218, 3468-3477 doi:10.1242/jeb.129486

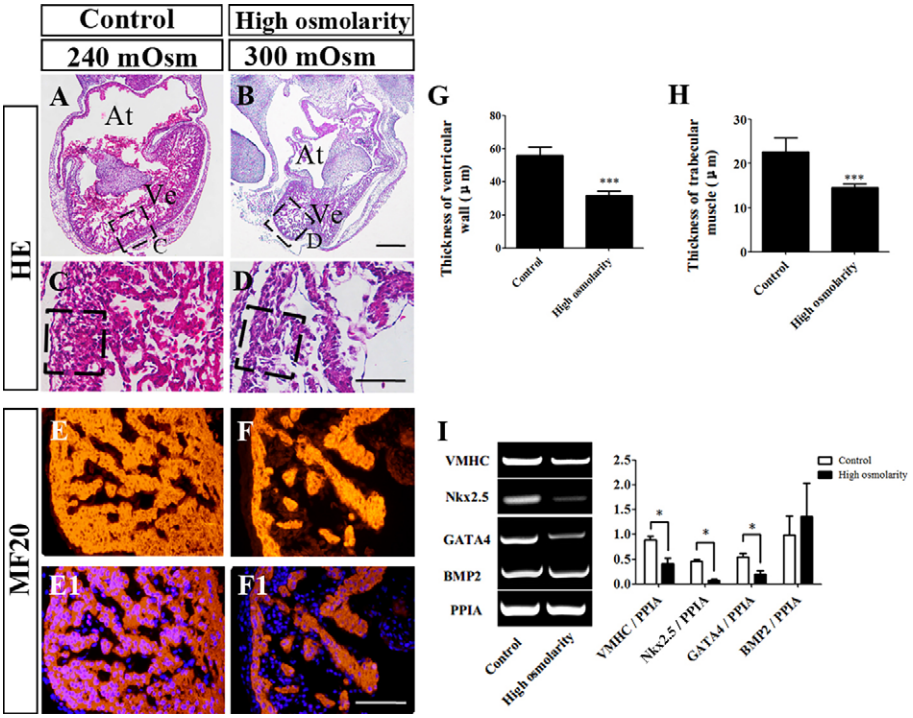

Fig. 3. High-salt exposure limits ventricular wall development in E4.5 chick embryos. Fertilized chick eggs were exposed to 0.7% NaCl (control) and 300 mOsm l^{-1} NaCl (high salt) for 3 days as described above. Transverse sections of hearts were stained with H&E, and representative images from control (A) and high salt-exposed (B) hearts were taken at the same spatial position. (C,D) High-magnification images were taken from the sites indicated by boxed regions in A and B, respectively. (E,F) MF20 immunofluorescent staining was performed on serial slices as shown in C and D, respectively. (E1,F1) Merged images of MF20 immunofluorescence and DAPI staining. (G) Bar graph comparing the ventricular wall thickness of control and high-salt-exposed hearts. (H) Bar graph comparing the trabecular muscle layers. (I) Semi-quantitative RT-PCR detection of *BMP2*, *Nkx2.5*, *VMHC* and *GATA4* mRNA expression in developing chick hearts after high osmolarity treatment. At, atrium; Ve, ventricle. Scale bars: 250 μm (A,B), 100 μm in (C,D), 100 μm in (E–F1).

in control embryos (Fig. 5C,E). The difference in PH3-positive cells was not due to absolute cell number differences in sections, as it was divided by the total cell number stained by DAPI (control=70.01±16.08%, N=10; high osmolarity=51.69±14.37%, N=8; P<0.01; Fig. 5G). Because Cyclin D1 regulates cell cycle progression, we determined the expression of Cyclin D1 mRNA using RT-PCR. Cyclin D1 was down-regulated in the presence of high salt (control=0.98±0.12, high osmolarity=0.26±0.10, N=4; P<0.05; Fig. 5H), further indicating that cell proliferation was repressed by exposure to high salt. However, as observed in heart formation, cell apoptosis as labeled by TUNEL staining was enhanced in the presence of high salt (control=23.29±16.08, high osmolarity=53.99±14.37, N=8, respectively; P<0.05; Fig. 5I–K).

The formation of blood islands in the extraembryonic region is repressed by high-salt exposure

The blood vessels in the yolk sac membrane are directly derived from blood islands in the extraembryonic area opaca at an early developmental stage. We therefore determined whether the inhibitive effect of high-salt exposure occurred at the earlier stage of blood island formation using early chick embryos. To avoid deviations in individual embryonic development, we exposed one

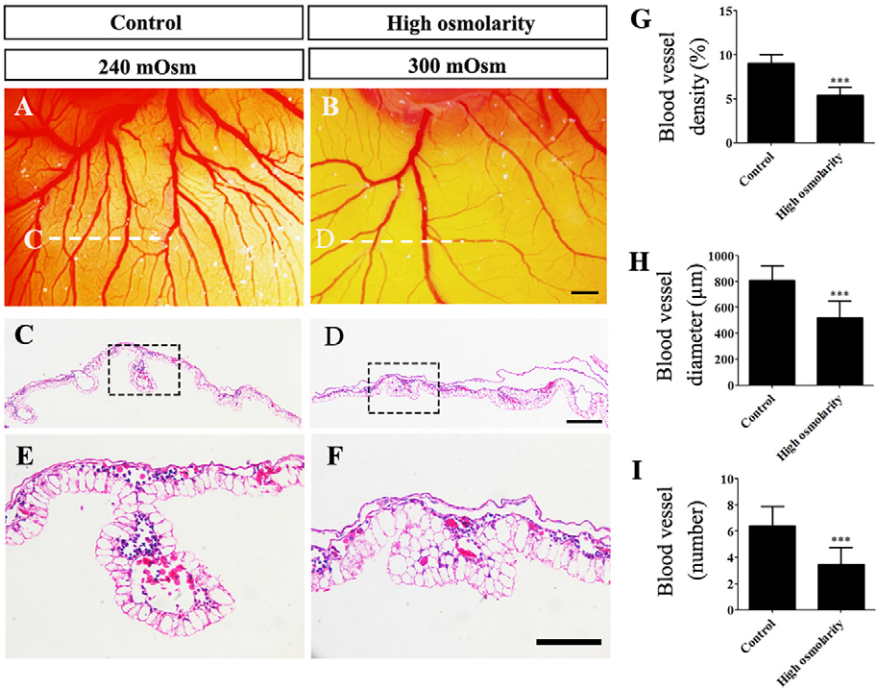

Fig. 4. High osmolarity restricts angiogenesis in the yolk sac membrane of E4.5 chick embryos. Fertilized chick eggs were exposed to high salt for 3 days. Representative images of the YSM vascular plexus in control (A) and high osmolarity (B) embryos derived from the same location relative to the E4.5 embryos. H&E stained transverse sections of the vascular plexus from control (C) and high osmolarity (D) YSM were taken at the sites indicated by white dotted lines in A and B, respectively. (E,F) High-magnification images taken from the sites indicated by boxes in C and D, respectively. (G) Bar graphs comparing (G) blood vessel density, (H) blood vessel diameter and (I) blood vessel number in the control and high-salt groups. ***P<0.001 indicates a significant difference between control and high osmolarity groups. Scale bars: 1 mm (A,B), 200 μm (C,D) and 100 μm (E,F).

Journal of Experimental Biology (2015) 218, 3468-3477 doi:10.1242/jeb.129486

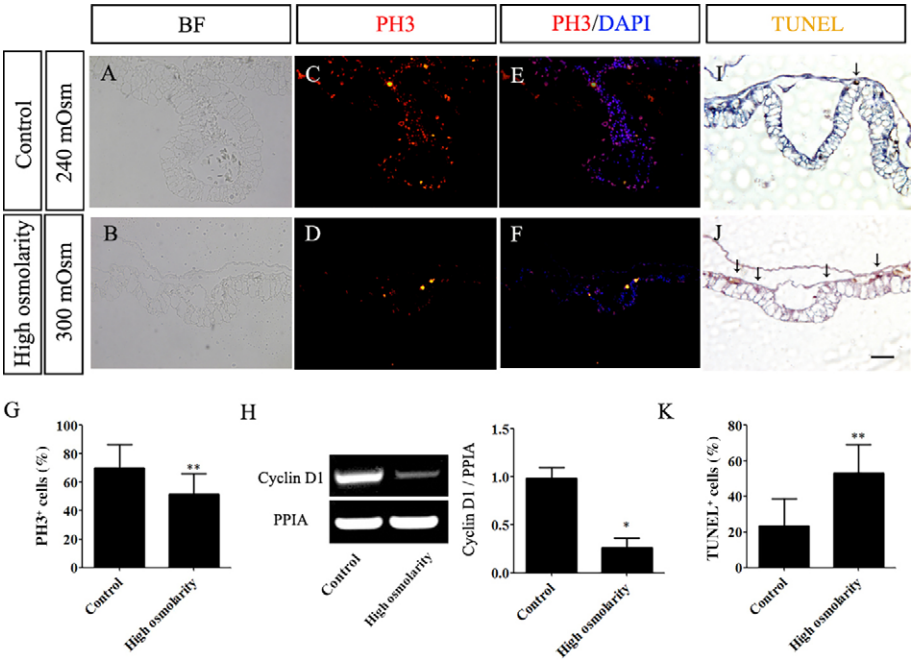

Fig. 5. High-salt exposure impacts cell proliferation and apoptosis in the yolk sac membrane vascular plexus in E4.5 chick embryos. Apoptosis and cell cycle profile were analyzed with TUNEL immunocytochemistry and PH3 immunofluorescent staining, respectively, on serial transverse sections as in Fig. 4. (A,B) Representative bright-field images of the YSM transverse sections from control and high osmolarity groups. (C,D) Representative images of PH3 immunofluorescent staining in YSM transverse sections. (E,F) Representative merged images of PH3 immunofluorescent staining with DAPI in the YSM transverse sections. (I,J) Representative TUNEL staining images in the YSM transverse sections. (G) Bar graph comparing the number of PH3-positive cells in the control and high osmolarity groups. (H) Semi-quantitative RT-PCR showing cyclin D1 mRNA expression in the YSM vascular plexus after high osmolarity treatment. Bar graph shows relative cyclin D1 expression in the control and high osmolarity groups. (K) Bar graph comparing the number of TUNEL-positive cells in the control and high osmolarity groups. **P*<0.05 and ***P*<0.01 indicate significant differences between experimental and control embryos. Scale bars: 50 μm (A–F,I,J).

side of the embryo to high salt, while the other side acted as a control (Fig. 6A). VE-cadherin *in situ* hybridization was performed in these treated chick embryos (Fig. 6B) because VE-cadherin is specifically expressed in blood islands in early stage embryos. Blood islands were clearly labeled with VE-cadherin in the area opaca, so we could observe and compare the blood island density (Fig. 6C,D) and numbers in transverse sections (Fig. 6E,F). The blood island density in high-salt-exposed embryos was reduced compared with control

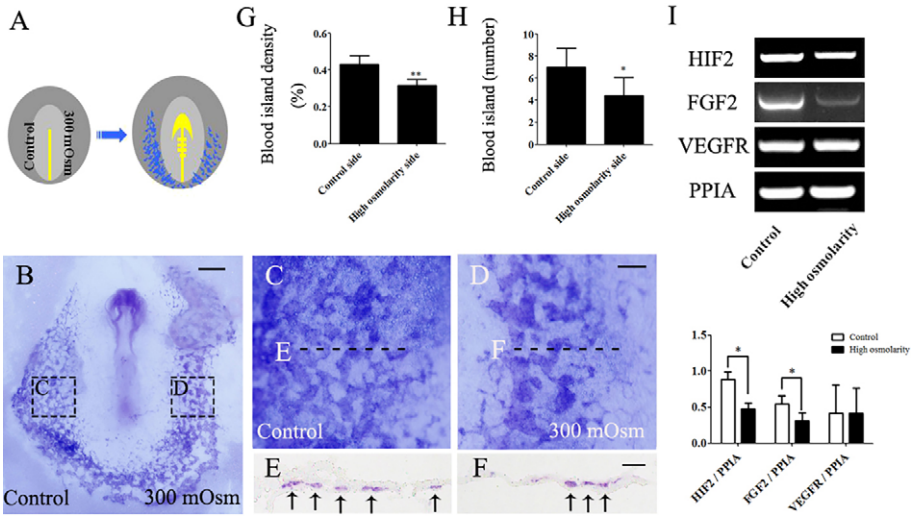

Fig. 6. High-salt exposure inhibits the development of blood islands in early stage embryos. (A) Chick embryos were exposed to 0.7% NaCl (control, left) and 300 mOsm l^{-1} NaCl (high osmolarity, right) using homemade 35 mm culture dishes isolated at the middle line for 12 h. (B) *In situ* hybridization of VE-cadherin was performed in chick embryos exposed to high salt on one half. (C,D) High-magnification images from control and high osmolarity sides as indicated by squares in B. (E,F) Transverse sections at the sites indicated by dashed lines in C and D, respectively. The blood islands are indicated by arrows. Bar graphs comparing (G) the blood island densities and (H) blood island numbers of the control and high osmolarity groups. (I) Semi-quantitative RT-PCR was performed to detect thshowing *HIF2*, *FGF2* and *VEGFR* mRNA expression in the area opaca of early chick embryos after the high osmolarity treatment. Bar graph comparing HIF2, FGF2 and VEGFR expressions in the control and high osmolarity groups is shown below. **P*<0.05 and ***P*<0.01 indicate significant differences between experimental and control embryos. Scale bars: 600 μm (B), 100 μm (C,D) and 200 μm (E,F).

Journal of Experimental Biology

Journal of Experimental Biology (2015) 218, 3468-3477 doi:10.1242/jeb.129486

embryos (control=43.18±4.74%, high osmolarity=31.59±3.32%, *N*=6 embryos, respectively, *P*<0.01; Fig. 6G). The number of blood islands was also reduced in the presence of high salt (control=7.00±1.63, high osmolarity=4.43±1.62, *N*=7 sections from three embryos, respectively, *P*<0.05; Fig. 6H). These data suggest that blood island formation was also inhibited by the exposure of high salt and that the inhibitive effect on angiogenesis by exposure to high salt occurs at an early stage.

The expression of well-known angiogenesis-related genes following high-salt treatment also supports these experimental observations. We measured the expression of *HIF2*, *FGF2* and *VEGFR* mRNA using RT-PCR in YSM samples. *HIF2* and *FGF2*, but not *VEGFR*, were down-regulated in the presence of high salt. A parallel test for PPIA confirmed that equal amounts of RNA were used in the RT reaction (*HIF2*/*PPIA*: control=0.89±0.10, high osmolarity=0.48±0.08, *P*<0.05; *FGF2*/*PPIA*: control=0.54±0.12, high osmolarity=0.31±0.11, *P*<0.05; *VEGFR*/*PPIA*: control=0.42±0.38, high osmolarity=0.41±0.35, *P*>0.05; *N*=4, respectively; Fig. 6I).

Similar inhibitory effects of high-salt exposure on angiogenesis were observed in the CAM

To confirm our observation of the high-salt effect on angiogenesis, we studied the CAM model, another well-known angiogenesis model. The embryos were exposed to a high-salt environment through the injection of either simple saline (500 µl of 0.7% salt solution) or high-salt solution (500 µl of 16.85% salt solution) from day 6 to day 8 (Fig. 7A). On day 8, we photographed and analyzed the CAM angiogenesis in the control (Fig. 7B) and high-salt-exposed (Fig. 7C) embryos. Blood vessel density was measured by appearance and analysis using specific software (control=10.01±0.60%, high osmolarity=7.23±0.58%, *N*=6 embryos, respectively, *P*<0.01; Fig. 7H). Moreover, the high-magnification images and the transverse sections from control and high-osmolarity groups showed that blood vessel density was reduced in the presence of high salt compared with the control (Fig. 7D–G). Altogether, the data from both angiogenesis models revealed that a high-salt environment significantly suppressed angiogenesis at different developmental stages.

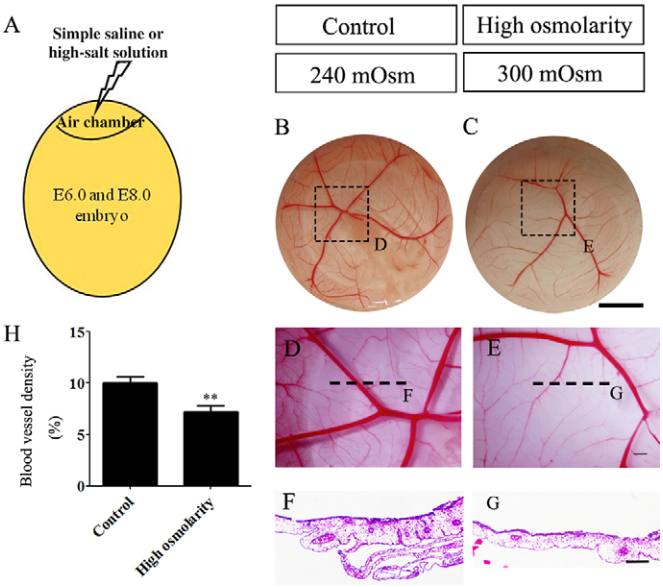

Fig. 7. Angiogenesis in the CAM is adversely affected by high-salt exposure. (A) E6 chick eggs were exposed to 0.7% NaCl (control) and 300 mOsm l^{-1} NaCl (high osmolarity) for 2 days. (B,C) Representative appearance of CAM from control and high osmolarity exposure. (D,E) High-magnification images from boxed regions in B and C, respectively. (F,G) Transverse sections at the sites indicated by black dotted lines in D and E, respectively. (H) Bar graph comparing the blood vessel densities of the control and high osmolarity groups. ***P*<0.01 indicates a significant difference between experimental and control embryos. Scale bars: 10 mm (B,C), 1 mm (D,E) and 200 µm (F,G).

Excess ROS generation is involved in high-salt-induced embryonic cardiovascular dysplasia

In our previous studies, excess reactive oxygen species (ROS) generation played an important role in angiogenesis defects (Jin et al., 2013; Li et al., 2014; Wang et al., 2015b). Therefore, we next studied the effect of excess ROS generation. Our results showed that ROS production was significantly increased in HUVECs after high-salt treatment (control=32.24±20.30%, high osmolarity=71.15±8.41%; *N*=6 in control group and *N*=6 in high-salt group, *P*<0.01; Fig. 8A). Because they are crucial genes encoding antioxidant enzymes, *GPx*, *SOD1* and *SOD2* expression could indicate the ROS generation activity. Using RT-PCR assay, we detected the mRNA expression of *GPx*, *SOD1* and *SOD2* in the developing heart (*Gpx*/*PPIA*: control=0.38±0.11, high osmolarity=1.48±0.32; *SOD1*/*PPIA*: control=0.79±0.06, high osmolarity=1.68±0.14; *SOD2*/*PPIA*: control=0.80±0.09, high osmolarity=1.46±0.16; Fig. 8B) and yolk sac membrane (*Gpx*/*PPIA*: control=0.28±0.10, high osmolarity=0.74±0.27; *SOD1*/*PPIA*: control=0.69±0.11, high osmolarity=0.98±0.20; *SOD2*/*PPIA*: control=0.46±0.11, high osmolarity=0.85±0.23; Fig. 8C) tissues following the high-salt treatment.

Excess ROS generation in tissues and cells is cytotoxic. However, it is not necessarily an essential component of the high-salt-induced cardiovascular development defects. To study this correlation, vitamin C, an antioxidant compound, was added together with high salt and development was observed. The embryonic mortality was reduced to some extent when the vitamin C was added (high osmolarity=70%, high osmolarity+Vc=50%, *N*=50 embryos in these two groups; Fig. 8D). The morphological observation of angiogenesis in the YSM also showed that addition of vitamin C (Fig. 8E) significantly rescued the reduction in blood vessel density in YSMs (control=9.21±0.89%, *N*=9; high osmolarity=5.07±1.34%, *N*=10; high osmolarity+Vc=7.59±2.02, *N*=8; *P*<0.05 between control and high osmolarity group; *P*<0.05 between high osmolarity+Vc and high osmolarity group; Fig. 8F–H).

We next determined the expression of *VMHC*, *Nkx2.5* and *GATA4* in heart tissue after the addition of vitamin C and found that the reduced expression after high-salt exposure was significantly rescued (*VMHC*/*PPIA*: control=1.22±0.11, high osmolarity=0.68± 0.07, high osmolarity+Vc=0.90±0.04; *Nkx2.5*/*PPIA*: control=1.17± 0.52, high osmolarity=0.29±0.20, high osmolarity+Vc=0.89±0.25; *GATA4*/*PPIA*: control=0.92±0.09, high osmolarity=0.34±0.19, high osmolarity+Vc=0.62±0.12; *P*<0.05; *N*=4, respectively; Fig. 8I). To assess angiogenesis-related gene expression, we measured *HIF2* and *FGF2* expression in YSM tissues after the addition of vitamin C using RT-PCR and found that the reduction in *HIF2* and *FGF2* expression induced by exposure to high salt was dramatically reversed in the rescued group (*HIF2*/*PPIA*: control=0.71±0.20, high osmolarity=0.43±0.05, high osmolarity+Vc=0.63±0.09; *FGF2*/*PPIA*: control=0.18±0.01, high osmolarity=0.09±0.03, high osmolarity+Vc=0.18±0.02; *P*<0.05; *N*=4, respectively; Fig. 8J). These experimental data suggest that excess ROS generation is involved in the high-salt-induced defects in cardiovascular development.

Journal of Experimental Biology

Journal of Experimental Biology (2015) 218, 3468-3477 doi:10.1242/jeb.129486

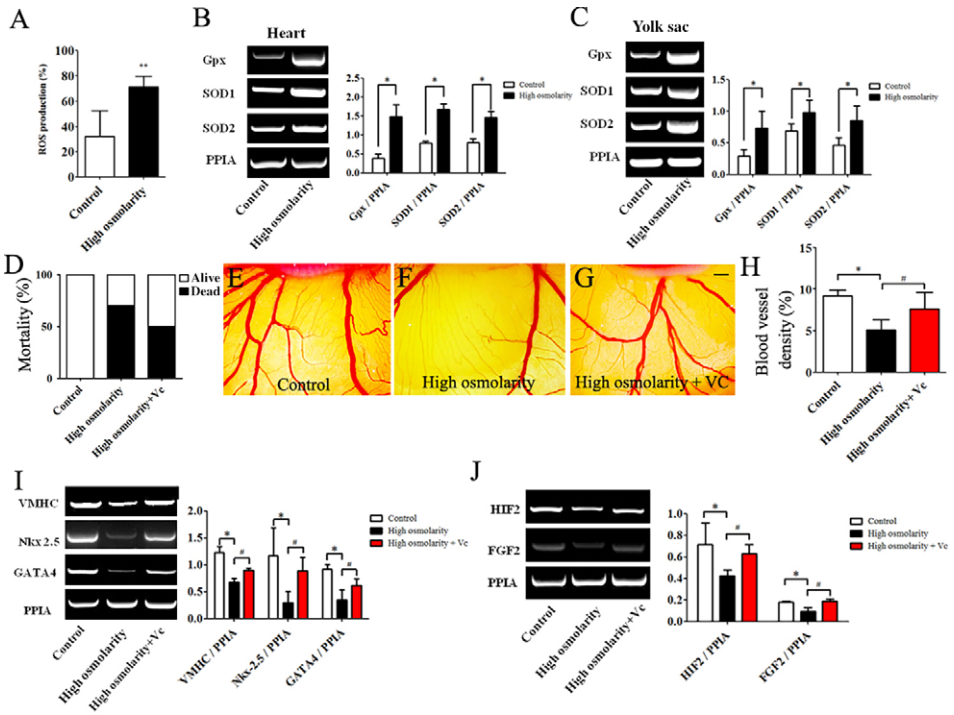

Fig. 8. Excess ROS are generated in developing hearts, YSM and CAM following high-salt exposure. (A) Bar chart comparing HUEVC proliferative rates (%) in control and high-salt-treated groups. (B) Semi-quantitative RT-PCR was performed to detect the mRNA expression of *Gpx*, *SOD1* and *SOD2* in the E4.5 developing hearts after high-salt exposure. Bar graph compares *Gpx*, *SOD1* and *SOD2* expression in the control and high osmolarity groups. (C) Semi-quantitative RT-PCR detects the mRNA expression of *Gpx*, *SOD1* and *SOD2* in the E4.5 embryonic yolk sacs after high-salt exposure. The right bar graph compares *Gpx*, *SOD1* and *SOD2* expression in the control and high osmolarity groups. (D) Bar graph comparing embryonic mortality among the control, high osmolarity and high osmolarity+vitamin C (Vc) groups. (E–G) Representative appearance of CAM in the control group, high osmolarity and high osmolarity+ vitamin C groups. (H) Bar graph comparing blood vessel densities. (I) Semi-quantitative RT-PCR and bar graph show mRNA expression of *VMHC*, *Nkx2.5* and *GATA4* in E4.5 embryonic hearts. (J) Semi-quantitative RT-PCR and bar graph compares mRNA expression of *HIF2* and *FGF2* in the E4.5 embryonic yolk sacs. *P<0.05 indicates significant differences between high osmolarity and control groups, $^{\#}P$<0.05 indicate significant differences between high osmolarity and high osmolarity+vitamin C groups. Scale bars: 1 mm (E–G).

DISCUSSION

In our study, We firstly observed the heart phenotypes in chick embryos after 4.5 days of high-salt exposure (Fig. 1C,D). Abnormal heart tube looping (Fig. 1C) and blood congestion within the heart cavity were detected in surviving embryos (Fig. 1D). In their corresponding transverse sections, the normal overturn of the developing atrium and ventricle was not yet completed compared with controls (Fig. 1B1–C3), and red blood cells filled the heart chamber (Fig. 1D1–3). Meanwhile, cardiomyocyte cell proliferation and apoptosis were also disturbed by high-salt exposure (Fig. 2). The cardiac transcription factors Nkx2.5 and GATA4 play important roles in vertebrate cardiac development. *Nkx2.5* and *GATA4* were initially identified as the genes causing congenital heart disease (Granados-Riveron et al., 2012; Wang et al., 2007). *Nkx2.5* and *GATA4* expression was dramatically reduced by high-salt exposure (Fig. 3I), indicating that high levels of salt interfered with the expression of these crucial heart formation genes. It is probably because of this inhibition that the MF20 was not completely expressed, indicating suppression of cardiomyocyte differentiation (Fig. 3E,F).

The accomplishment of cardiovascular functions relies on an integrated heart–blood vessel system. The pathological cardiovascular development phenotypes may also result from defective vascular development. Therefore, we investigated angiogenesis in the presence of high salt using chick YSM and CAM models, which have been extensively employed for studying angiogenesis (He et al., 2014; Mitashev et al., 2001). Vessel formation in the YSM includes vasculogenesis at early stages and angiogenesis at later stages, including the specification of the migrating mesoderm-derived hemangioblasts, the primary and secondary sprouting of intersomitic vessels and arterial versus venous modeling (Baldessari and Mione, 2008).

In this study, we revealed that the number, density and diameter of blood vessels were suppressed by exposure to high salt in both the YSM and CAM models (Figs 4 and 7). Because blood island formation occurs in the area opaca where the initial angiogenesis also occurs, we determined whether high-salt exposure affected blood island formation and vasculogenesis (Fig. 6). High-salt exposure suppressed blood island formation, suggesting that the high-salt-induced suppression of angiogenesis occurred at different stages of angiogenesis. Angiogenesis is a strictly regulated process, balancing stimulatory and inhibitory factors to control the correct development of blood vessels. Well-characterized angiogenic and angiostatic factors such as HIF-1, AP-1 and Sp-1 modulate angiogenesis by regulating VEGF expression (Josko and Mazurek, 2004). We measured cell proliferation and apoptosis using PH3 and TUNEL staining in the transverse sections of YSM blood vessels and showed that cell proliferation was suppressed and apoptosis was enhanced by high-salt exposure (Fig. 5A–J). The consequent reduction in cyclin D1 expression also supported the inactivation of the cell cycle by exposure to high salt (Fig. 5H). Fibroblast growth factor-2 (FGF2) is in the FGF family. FGF2 exerts its angiogenic activity by interacting with endothelial cell surface receptors including tyrosine kinase receptors, heparan sulfate

Journal of Experimental Biology (2015) 218, 3468-3477 doi:10.1242/jeb.129486

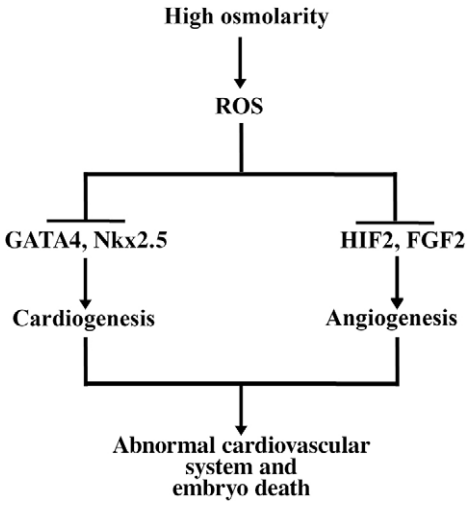

Fig. 9. Proposed summary of the mechanism by which high-salt exposure causes cardiovascular dysplasia during embryonic development.

proteoglycans and integrins (Presta et al., 2009). In this study, RT-PCR data showed that FGF2 expression was down-regulated by high-salt exposure (Fig. 6I). These data suggest that high-salt-suppressed angiogenesis might be due to the negative regulation of HIF2 and FGF2, but not VEGFR expression. What we need to keep in mind is that VEGF itself is not deemed to be efficient, although it does plays a crucial role in vascularization. Therefore, other growth factors/cytokines, including angiopoietins, SDF-1, PDGFb and FGF2 etc. are also involved in sprouting angiogenesis (Cao et al., 2003; Thurston et al., 1999). Further experiments are still required to address this question.

As a natural byproduct of aerobic metabolism, ROS play an important role in cell signaling and homeostasis. However, excess ROS might result in significant damage to cell structures (Devasagayam et al., 2004). Whether ROS will cause damage or act as a signaling molecule depends on the delicate balance between ROS production and elimination. It was reported that embryonic dysmorphogenesis is blocked by adding an antioxidant *in vivo* and *in vitro*, suggesting that excess ROS in embryonic tissues activate the teratogenic process of diabetic pregnancy (Forsberg et al., 1998). Similar results on excess ROS generation were also observed in our study (Fig. 8A). Moreover, the RT-PCR data indicated that GPx, SOD1 and SOD2 expression dramatically increased in both the heart tube and yolk sac membrane following high-salt treatment (Fig. 8B,C), suggesting that excess ROS were generated there. Meanwhile, the high embryonic mortality was partially rescued by the addition of vitamin C, an antioxidant (Fig. 8D). The partial rescue effect was also observed in blood vessel developmental morphology (Fig. 8E–G). To further investigate the effect of antioxidants in oxidation stress, we detected the expression of key genes in heart tube formation and angiogenesis using an RT-PCT assay and showed that *VMHC*, *Nkx2.5* and *GATA4* expression in the antioxidant group rebounded from the level of high-salt-suppressed gene expression in heart tubes (Fig. 8I). Similarly, *HIF2* and *FGF2* expression in the YSM of the antioxidant group was also rescued to some extent (Fig. 8J).

Altogether, our data suggest that the embryonic cardiovascular dysplasia due to high osmolarity exposure from high salt might result from defects in heart formation and angiogenesis, respectively. Moreover, the excess ROS generation due to high-salt exposure could interfere with expression of genes involved in heart development (*Nkx2.5* and *GATA4*) and angiogenesis (*HIF2* and *FGF2*). Consequently, the abnormal looping of heart tube and blood congestion in developing heart emerges, as illustrated in Fig. 9. Further experimental studies on signaling pathways are required to explore the precise molecular biological mechanisms.

Acknowledgements
We would like to thank Dr Zhi Huang for providing the HUVECs.

Competing interests
The authors declare no competing or financial interests.

Author contributions
G.W., N.Z., Y.-F.W., Y.-M.J., S.-Y.Z., X.C., Z.-L.M. and S.-Z.Z. performed the experiments and collected the data; G.W., Y.-P.C., M.C., B.H. and X.Y. designed the study and analyzed the data; X.Y. wrote the manuscript.

Funding
This study was supported by NSFC grant (81571436; 31401230); Medical Scientific Research Foundation of Guangdong Province (A2015201); Science and Technology Program of Guangzhou (201510010073); China Postdoctoral Science Foundation (2015T80940; 2014M560694); the Fundamental Research Funds for the Central Universities (21614319, 21615421); The Funds for Young Creative Talents of Higher Education in Guangdong Province (2014KQNCX026) and Students Research Training Program Fund (201410559032, 1210559035, CX13181).

References
Baldessari, D. and Mione, M. (2008). How to create the vascular tree? (Latest) help from the zebrafish. *Pharmacol. Ther.* **118**, 206-230.
Brand, T. (2003). Heart development: molecular insights into cardiac specification and early morphogenesis. *Dev. Biol.* **258**, 1-19.
Brown, D. I. and Griendling, K. K. (2015). Regulation of signal transduction by reactive oxygen species in the cardiovascular system. *Circ. Res.* **116**, 531-549.
Cao, R., Brakenhielm, E., Pawliuk, R., Wariaro, D., Post, M. J., Wahlberg, E., Leboulch, P. and Cao, Y. (2003). Angiogenic synergism, vascular stability and improvement of hind-limb ischemia by a combination of PDGF-BB and FGF-2. *Nat. Med.* **9**, 604-613.
Chapman, S. C., Collignon, J., Schoenwolf, G. C. and Lumsden, A. (2001). Improved method for chick whole-embryo culture using a filter paper carrier. *Dev. Dyn.* **220**, 284-289.
Chen, Y., Wang, G., Wang, X. Y., Ma, Z. L., Chen, Y. P., Chuai, M., von Websky, K., Hocher, B. and Yang, X. (2014). Effects of high salt-exposure on the development of retina and lens in 5.5-day chick embryo. *Cell Physiol. Biochem.* **34**, 804-817.
De Simone, R., Ajmone-Cat, M. A., Carnevale, D. and Minghetti, L. (2005). Activation of alpha7 nicotinic acetylcholine receptor by nicotine selectively up-regulates cyclooxygenase-2 and prostaglandin E2 in rat microglial cultures. *J. Neuroinflamm.* **2**, 4.
Dennery, P. A. (2007). Effects of oxidative stress on embryonic development. *Birth Defects Res. C Embryo Today* **81**, 155-162.
Devasagayam, T. P., Tilak, J. C., Boloor, K. K., Sane, K. S., Ghaskadbi, S. S. and Lele, R. D. (2004). Free radicals and antioxidants in human health: current status and future prospects. *J. Assoc. Phys. India* **52**, 794-804.
Dugaiczyk, A., Haron, J. A., Stone, E. M., Dennison, O. E., Rothblum, K. N. and Schwartz, R. J. (1983). Cloning and sequencing of a deoxyribonucleic acid copy of glyceraldehyde 3-phosphate dehydrogenase messenger ribonucleic acid isolated from chicken muscle. *Biochemistry* **22**, 1605-1613.
Endo, Y., Ishiwata-Endo, H. and Yamada, K. M. (2012). Extracellular matrix protein anosmin promotes neural crest formation and regulates FGF, BMP, and WNT activities. *Dev. Cell* **23**, 305-316.
Forsberg, H., Eriksson, U. J., Melefors, O. and Welsh, N. (1998). Beta-hydroxybutyrate increases reactive oxygen species in late but not in early postimplantation embryonic cells in vitro. *Diabetes* **47**, 255-262.
Granados-Riveron, J. T., Pope, M., Bu'lock, F. A., Thornborough, C., Eason, J., Setchfield, K., Ketley, A., Kirk, E. P., Fatkin, D., Feneley, M. P. et al. (2012). Combined mutation screening of NKX2–5, GATA4, and TBX5 in congenital heart disease: multiple heterozygosity and novel mutations. *Congenit. Heart Dis.* **7**, 151-159.
Hagen, T. (2012). Oxygen versus reactive oxygen in the regulation of HIF-1alpha: the balance tips. *Biochem. Res. Int.* **2012**, 436981.
He, R.-R., Li, Y., Li, X.-D., Yi, R.-N., Wang, X.-Y., Tsoi, B., Lee, K. K. H., Abe, K., Yang, X. and Kurihara, H. (2013). A new oxidative stress model, 2,2-azobis(2-

amidinopropane) dihydrochloride induces cardiovascular damages in chicken embryo. *PLoS ONE* **8**, e57732.
He, Y.-Q., Li, Y., Wang, X.-Y., He, X.-D., Jun, L., Chuai, M., Lee, K. K. H., Wang, J., Wang, L.-J. and Yang, X. (2014). Dimethyl phenyl piperazine iodide (DMPP) induces glioma regression by inhibiting angiogenesis. *Exp. Cell Res.* **320**, 354-364.
Henrique, D., Adam, J., Myat, A., Chitnis, A., Lewis, J. and Ish-Horowicz, D. (1995). Expression of a Delta homologue in prospective neurons in the chick. *Nature* **375**, 787-790.
Jin, Y.-M., Zhao, S.-Z., Zhang, Z.-L., Chen, Y., Cheng, X., Chuai, M., Liu, G.-S., Lee, K. K. H. and Yang, X. (2013). High glucose level induces cardiovascular dysplasia during early embryo development. *Exp. Clin. Endocrinol. Diabetes* **121**, 448-454.
Jin, Y.-M., Wang, G., Zhang, N., Wei, Y.-F., Li, S., Chen, Y.-P., Chuai, M., Lee, H. S. S., Hocher, B. and Yang, X. (2015). Changes in the osmolarity of the embryonic microenvironment induce neural tube defects. *Mol. Reprod. Dev.* **82**, 365-376.
Josko, J. and Mazurek, M. (2004). Transcription factors having impact on vascular endothelial growth factor (VEGF) gene expression in angiogenesis. *Med. Sci. Monit.* **10**, RA89-RA98.
Larger, E., Marre, M., Corvol, P. and Gasc, J.-M. (2004). Hyperglycemia-induced defects in angiogenesis in the chicken chorioallantoic membrane model. *Diabetes* **53**, 752-761.
Li, Y., Wang, X.-Y., Zhang, Z.-L., Cheng, X., Li, X.-D., Chuai, M., Lee, K. K. H., Kurihara, H. and Yang, X. (2014). Excess ROS induced by AAPH causes myocardial hypertrophy in the developing chick embryo. *Int. J. Cardiol.* **176**, 62-73.
Linask, K. K. (2003). Regulation of heart morphology: current molecular and cellular perspectives on the coordinated emergence of cardiac form and function. *Birth Defects Res. C Embryo Today* **69**, 14-24.
Marinaccio, C., Nico, B. and Ribatti, D. (2013). Differential expression of angiogenic and anti-angiogenic molecules in the chick embryo chorioallantoic membrane and selected organs during embryonic development. *Int. J. Dev. Biol.* **57**, 907-916.
Maroto, M., Reshef, R., Munsterberg, A. E., Koester, S., Goulding, M. and Lassar, A. B. (1997). Ectopic Pax-3 activates MyoD and Myf-5 expression in embryonic mesoderm and neural tissue. *Cell* **89**, 139-148.
Mitashev, V. I., Koussoulakos, S., Zinov'eva, R. D., Ozerniuk, N. D., Mikaelian, A. S., Shmukler, E. and Smirnova Iu, A. (2001). [Constructive synergism of regulatory genes expressed in the course of the eye and muscle development and regeneration]. *Izv. Akad. Nauk Ser. Biol.* **3**, 261-275.
Nakajima, Y., Sakabe, M., Matsui, H., Sakata, H., Yanagawa, N. and Yamagishi, T. (2009). Heart development before beating. *Anat. Sci. Int.* **84**, 67-76.
Patan, S. (2004). Vasculogenesis and angiogenesis. *Cancer Treat. Res.* **117**, 3-32.
Presta, M., Andres, G., Leali, D., Dell'Era, P. and Ronca, R. (2009). Inflammatory cells and chemokines sustain FGF2-induced angiogenesis. *Eur. Cytokine Netw.* **20**, 39-50.
Pugh, C. W. and Ratcliffe, P. J. (2003). Regulation of angiogenesis by hypoxia: role of the HIF system. *Nat. Med.* **9**, 677-684.
Schlueter, J., Manner, J. and Brand, T. (2006). BMP is an important regulator of proepicardial identity in the chick embryo. *Dev. Biol.* **295**, 546-558.
Schultheiss, T. M., Xydas, S. and Lassar, A. B. (1995). Induction of avian cardiac myogenesis by anterior endoderm. *Development* **121**, 4203-4214.
Scott-Drechsel, D. E., Rugonyi, S., Marks, D. L., Thornburg, K. L. and Hinds, M. T. (2013). Hyperglycemia slows embryonic growth and suppresses cell cycle via cyclin D1 and p21. *Diabetes* **62**, 234-242.
Thurston, G., Suri, C., Smith, K., McClain, J., Sato, T. N., Yancopoulos, G. D. and McDonald, D. M. (1999). Leakage-resistant blood vessels in mice transgenically overexpressing angiopoietin-1. *Science* **286**, 2511-2514.
Wang, Y., Morishima, M., Zheng, M., Uchino, T., Mannen, K., Takahashi, A., Nakaya, Y., Komuro, I. and Ono, K. (2007). Transcription factors Csx/Nkx2.5 and GATA4 distinctly regulate expression of Ca2+ channels in neonatal rat heart. *J. Mol. Cell. Cardiol.* **42**, 1045-1053.
Wang, G., Huang, W. Q., Cui, S. D., Li, S., Wang, X. Y., Li, Y., Chuai, M., Cao, L., Li, J. C., Lu, D. X. et al. (2015a). Autophagy is involved in high glucose-induced heart tube malformation. *Cell Cycle* **14**, 772-783.
Wang, G., Zhong, S., Zhang, S. Y., Ma, Z. L., Chen, J. L., Lu, W. H., Cheng, X., Chuai, M., Lee, K. K., Lu, D. X. et al. (2015b). Angiogenesis is repressed by ethanol exposure during chick embryonic development. *J. Appl. Toxicol.* doi: 10.1002/jat.3201.
Xia, C., Meng, Q., Liu, L.-Z., Rojanasakul, Y., Wang, X.-R. and Jiang, B.-H. (2007). Reactive oxygen species regulate angiogenesis and tumor growth through vascular endothelial growth factor. *Cancer Res.* **67**, 10823-10830.
Yang, X., Chrisman, H. and Weijer, C. J. (2008). PDGF signalling controls the migration of mesoderm cells during chick gastrulation by regulating N-cadherin expression. *Development* **135**, 3521-3530.
Yutzey, K. E. and Kirby, M. L. (2002). Wherefore heart thou? Embryonic origins of cardiogenic mesoderm. *Dev. Dyn.* **223**, 307-320.
Zhang, H., Toyofuku, T., Kamei, J. and Hori, M. (2003). GATA-4 regulates cardiac morphogenesis through transactivation of the N-cadherin gene. *Biochem. Biophys. Res. Commun.* **312**, 1033-1038.